A METHODOLOGY FOR THE CALIBRATION OF SPHERICAL INDENTERS

J. G. Swadener and G. M. Pharr

The University of Tennessee, Dept. of Materials Science & Engr. , Knoxville, TN 37996-2200
and Oak Ridge National Laboratory, Metals and Ceramics Division

ABSTRACT

Spherical indentation with continuous load and depth measurement is a useful technique for characterizing thin film mechanical properties. With this technique, the initial loading is in the elastic range. Therefore the elastic-plastic transition can be observed. However, the calibration of spherical indenters presents special problems. First, the radius of the indenter at the point of contact must be determined, and any deviation from a spherical radius must be evaluated. The shape of the indenter also causes mounting difficulties that can create a relatively large and nonlinear compliance in the testing machine. The calibration of spherical indenters is further complicated, because asperities on the indenter and surface roughness add to the uncertainty in locating the surface of the sample. In addition, spherical indenters are generally made of anisotropic single crystals, and the calculation of their elastic responses must include this anisotropy. To address these issues, a methodology has been developed for the calibration of spherical indenters, whereby indentation experiments are conducted on multiple ceramic materials in the elastic range. The method was used to determine the local radius of synthetic sapphire spherical indenters. The accuracy of this measurement was verified using confocal microscopy. The method was successfully applied to an indenter with a nonlinear machine compliance. Further results involving indentation in the plastic regime are also presented.

INTRODUCTION

Nanoindentation has been shown to be a useful technique for characterizing the mechanical properties of materials and thin films in particular [1-3]. A spherical indenter has the special feature that the initial loading is in the elastic regime and that the transition from purely elastic to elastic-plastic deformation can be observed [4, 5]. However, the spherical shape that permits initially elastic loading presents difficulties in the calibration of the nanoindentation apparatus.

First, the location of the specimen surface is more difficult for a spherical indenter because of its relatively large contact area at small loads. Any asperities on the specimen surface or the tip of the indenter can give a false location of the surface. This problem can be circumvented by using unloading results in the elastic regime to determine the true surface location for the calibration, since the asperities are generally flattened during loading.

In addition, truly spherical tips with a predetermined radius are difficult to fabricate, so the actual radius of curvature at the point of contact must be determined in the calibration procedure. The mounting of the sphere presents additional manufacturing difficulties, which may lead to a nonlinear load-displacement response in the assembly. To complicate the

matter, the indenter radius and the compliance of the apparatus are coupled in the analysis. The calibration method presented below simultaneously determines the indenter radius and the compliance of the apparatus (machine compliance) by analyzing the results from two specimens with substantially different mechanical properties. A nonlinear machine compliance can be explicitly accommodated by the method.

A previous solution by Willis [6] or a recent simplification [7] can be used to account for anisotropy in the spherical indenter or in the specimens used for calibration. The calibration method can be readily applied, and results for a variety of materials are presented.

EXPERIMENT

Nanoindentation experiments were conducted with a 0.16 nm displacement resolution and a load resolution of 0.3 µN. The nanoindenter was used in continuous stiffness measurement mode with a 45 Hertz oscillation of 2 nm peak to peak. The indenter tips were fabricated from polished synthetic sapphire spheres with a nominal diameter of 130 µm. The spheres were pressed into stainless steel mounts and fixed in place by brazing or with an adhesive.

Four specimen materials were used in this study: polycrystalline 7075-T6 aluminum, fused quartz, synthetic sapphire, and silicon. The elastic moduli of these specimens are listed in Table 1. The fused quartz and synthetic sapphire were polished to optical standards. The silicon specimen was taken from a polished silicon wafer, and the aluminum specimen was mechanically polished with 0.1 µm diamond paste.

Table 1. Components of the Elastic Stiffness Matrix (GPa)

Material	C_{11}	C_{12}	C_{13}	C_{14}	C_{33}	C_{44}	reference
Aluminum	91	39	-	-	-	-	[8]
Fused Quartz	84	17.2	-	-	-	-	[9]
Sapphire	496.72	163.40	110.73	-23.49	499.98	147.40	[10]
Silicon	165.78	63.94	-	-	-	79.62	[11]

THEORY

In indentation experiments, the total measured displacement (h) can be divided into three parts: the deflection of the specimen surface (h_s), the deflection of the indenter surface (h_i) and the deflection of the apparatus (h_m), that is:

$$h = h_s + h_i + h_m . \tag{1}$$

For a contact that is small compared to the radius of the sphere, the deflections for the elastic contact of an isotropic spherical indenter and an isotropic flat specimen are given by the classical Hertz solution as:

$$h_s + h_i = \left(\frac{3P}{4E_{eff}\sqrt{R}} \right)^{\frac{2}{3}} , \tag{2}$$

where P is the applied load, R is the radius of the sphere and E_{eff} is the effective indentation modulus, which is given by:

$$\frac{1}{E_{eff}} = \frac{1-\nu_s^2}{E_s} + \frac{1-\nu_i^2}{E_i}, \tag{3}$$

where E_s and ν_s are the elastic modulus and Poisson's ratio respectively of the specimen and E_i and ν_i are the elastic modulus and Poisson's ratio respectively of the indenter. For anisotropic materials, E_{eff} is a complicated combination of all the components of the elastic stiffness matrix. A method to determine E_{eff} for anisotropic materials has been given by Willis [6]. A simplified formula for E_{eff} has recently been developed by Swadener and Pharr [7], but is not repeated here due to space limitations. The same results can be obtained through the more complicated procedure given by Willis [6].

Calibration experiments in the elastic regime can be performed to determine the total displacement over a range of load. Subtracting equation (2) from equation (1) gives h_m as a function of load:

$$h_m = h - \left(\frac{3P}{4E_{eff}\sqrt{R}}\right)^{\frac{2}{3}}. \tag{4}$$

RESULTS AND DISCUSSION

The radius of curvature at the tip of the spherical indenter and the displacement of the apparatus as a function of load are the two primary parameters to be determined by calibration. Calibration experiments in the elastic regime on two specimens with substantially different indentation moduli can be used to solve for h_m and R by equation (4). The value of R can be found by using a selected value of R in equation (4) to derive h_m from indentation experiments in two materials. The choice of R is then iterated until the plot of h_m as a function of load agrees for the two materials.

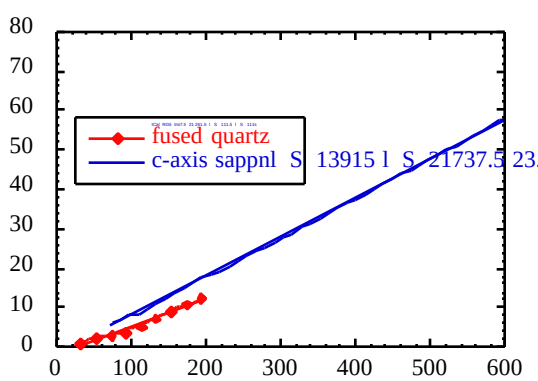

S 13915 l S 21737.5 23.5 201..5 l S 27ı. T(44.5 l Seriv201and tplain 27 in 0.5 l 5.5 l S 2890.5 l

An example of this calibration procedure is shown in Figures 1 and 2. A synthetic sapphire spherical indenter was used. The indentation modulus for sapphire has recently been determined to be within the range of 412-438 GPa for any orientation [7]. The median value (425 GPa) was used for these calculations. Initially a value of R = 65 µm gave a larger value for the machine compliance for the c-axis sapphire than for the fused quartz specimen (Fig. 1). Thechoice R = 69 µm gives as an approximately linear function of load in both fused quartz and c-axis sapphire (Fig. 2). The machine compliance (averaged over 5-10 experiments) for both materials is 0.11×10^{-6} m/N, which gives a machine stiffness of 9.0×10^{6} N/m. The indentation experiments for these two materials were conducted to different maximum loads (200 mN for fused quartz and 600 mN for sapphire) so that approximately the same contact depth (200 nm) was obtained in both materials. Conducting the experiments to the same contact depth has the advantage of using the same region on the spherical indenter whose radius is being determined.

After the radius of the sphere and the machine stiffness have been determined, indentation to different contact depths can show if the spherical radius is constant with depth. Two methods were used to calculate the effective indentation modulus from experiments on fused quartz. For both methods, a curve fit of the unloading curve was used in the data reduction. The Hertz method employed equations (1), (2) and (3) to determine E_{eff}, with h_m calculated from the machine compliance. The other method was that given by Oliver and Pharr [3]. Indentation modulus ($E / 1-\nu^2$) results for fused quartz were determined using a 69 µm spherical radius and a machine compliance of 9.0×10^{6} N/m and are plotted versus contact depth in Figure 3. For each set of experimental results, the average indentation modulus is within 5% of the analytical value (74.1 GPa), which indicates that the spherical radius is approximately constant over this range of contact depth. Indentation experiments were conducted on two additional materials to verify the calibration. Indentation modulus results for a [111] silicon surface are shown in Figure 4. The results are within 5% of the analytical value (175.4 GPa) and are approximately constant with depth. The indentation modulus values for aluminum were calculated using only the Oliver-Pharr method, because the Hertz

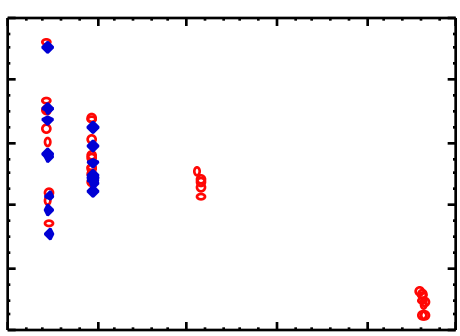

method only applies for elastic contact, and a large degree of plastic deformation occurred. The results for aluminum shown in Figure 5 agree with the prediction at moderate contact depths, but are low at small depths and somewhat high at large depths. The discrepancies are still under investigation, but may be due to depth dependent pile-up phenomena [see 12].

Sometimes, the machine compliance of spherical indenters will be nonlinear due to the way the sphere is mounted. In that case, the same calibration procedure can be applied by using a nonlinear curve fit for the machine displacement as a function of load. An example of a nonlinear machine compliance is shown in Figure 6. A cubic polynomial curve fit is used to match the experimental results for c-axis sapphire using a 57 µm spherical radius for this indenter. The results for fused quartz at the same indentation depth agreed with this machine compliance. For this indenter, the indentation modulus for fused quartz is shown in Figure 7 to be within 5% of the analytical value and approximately constant with depth. This indenter was also examined by confocal microscopy to evaluate deviations from the determined spherical radius. The projected surface area of the indenter is shown in Figure 8 to agree with the ideal result within 2% to a contact depth of 10 µm.

SUMMARY

For a nanoindentation system using a spherical indenter, a calibration procedure has been presented. The method entails performing indentation experiments on two ceramic materials to the same contact depth. The experimental results are then used to determine the radius of the spherical indenter and the machine compliance. The method has low sensitivity to surface asperities and was shown to give accurate results on several specimens. The calibration procedure was also extended to the case of a nonlinear machine compliance. For this case, the accuracy of the spherical radius determined by this method was verified by confocal microscopy measurements.

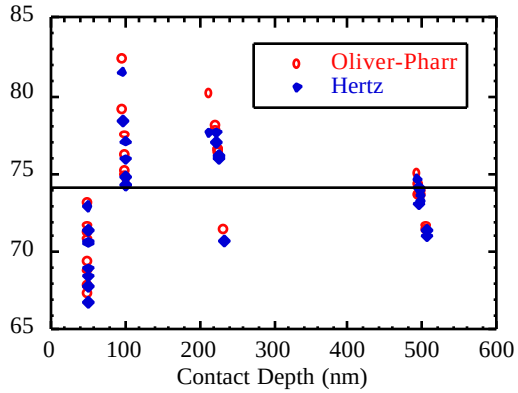

Figure 7. Indentation modulus of fused quartz from spherical indentation, R = 57 µm, cubic machine compliance from Fig. 6

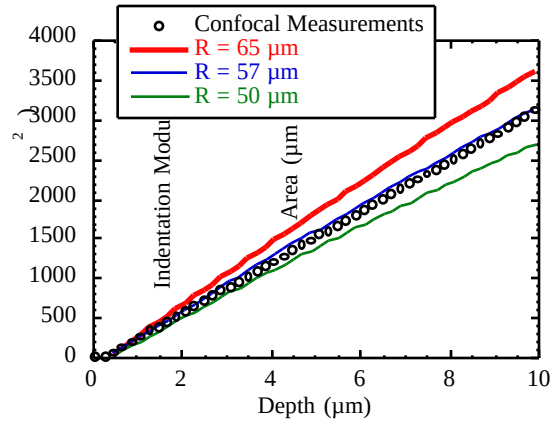

Figure 8. Projected surface area of a spherical indenter measured by confocal microscopy (◦) compared to perfect spheres (lines)

ACKNOWLEDGMENTS

The authors wish to thank Ms. Monica Schmidt for assistance with the confocal microscopy measurements. Research at the Oak Ridge National Laboratory SHaRE User Facility was sponsored by the Division of Materials Sciences, U.S. Department of Energy, under contract DE-AC05-96OR22464 with Lockheed Martin Energy Research Corp.

REFERENCES

1. J. B. Pethica, R. Hutchings and W. C. Oliver, Phil. Mag. A **48**, 593 (1983).
2. M. F. Doerner and W. D. Nix, J. Mater. Res. **1**, 601 (1986).
3. W. C. Oliver, and G. M. Pharr, J. Mater. Res. **7**, 1564 (1992).
4. H. A. Francis, J. Eng. Mater. Tech. **98**, 272 (1976).
5. J. S. Field and M. V. Swain, J. Mater. Res. **8**, 277 (1993).
6. J. R. Willis, J. Mech. Phys. Solids **14**, 163 (1966).
7. J. G. Swadener and G. M. Pharr, to be published.
8. The Aluminum Association, *Aluminum Standards and Data*, The Aluminum Association, New York, 1968, pp. 28-31.
9. General Electric Fused Quartz Products Technical Data, general catalog no. 7705-7725, April 1985.
10. J. B. Wachtman Jr., W. E. Tefft, D. C. Lam Jr., and R. P. Stenchfield, J. Res. NBS **64A**, (3), 213 (1960).
11. G. Simmons and H. Wang, *Single Crystal Elastic Constants and Calculated Aggregate Properties: A Handbook*, 2nd ed., MIT Press, Cambridge, MA, 1971, p. 85.
12. A. Bolshakov and G. M. Pharr, J. Mater. Res. **13**, 1049 (1998).